5ème Conférence Internationale des Energies Renouvelables (CIER– 2017)
Proceeding of Engineering and Technology –PET
Vol.27 pp.86-91

Performance analysis of hydrogen based heat driven single pressure absorption refrigeration machine for solar cooling

M. CHATTI [#], N. BEN EZZINE [#,*1], R. GARMA [#], A. BELLAGI [#2]

[#] *U.R. Thermique et Thermodynamique des Procédés Industriels,*
Ecole Nationale d'Ingénieurs de Monastir, Av. Ibn Jazzar, 5060 Monastir, Tunisia
[1] n_benezzine@yahoo.fr
[2] a.bellagi@enim.rnu.tn
[*] *Faculté des Sciences de Bizerte,*
Université de Carthage, 7021 Zarzouna, Tunisia

***Abstract*—**
Solar Absorption refrigeration is one of the most important method on utilizing thermal energy. In recent years, the research interest on hydrogen diffusion absorption refrigeration (HDAR) techniques has been increased significantly.
In this study, a detailed thermodynamic analysis of the hydrogen-ammonia-water diffusion absorption refrigeration machine is performed by numerical simulation.
The influences of driving heat temperature T_{max}, cooling medium temperature T_c , absorber effectiveness Eff_{abs} and concentration of ammonia solution on the thermal loads of components, on coefficients of performance COP, on minimum evaporation temperature and on the circulation ratio are investigated and discussed.
The performance characteristics of this system is analyzed parametrically by computer simulation with two cooling mediums, viz. water (27°C) and air (35°C). In the case of air-cooled machine with absorber effectiveness of 80%, the optimum driving temperature is around 140°C, and the corresponding *COP* reaching 0.22. In comparison, the performance of the water-cooled cycle is better with a lower optimum driving temperature around 120°C and a higher COP is up to 0.36.

***Keywords*— Modelling, Simulation, Coefficient of performance, Absorption, Refrigeration**

I. INTRODUCTION

In recent years, research has been devoted to improvement of absorption refrigeration systems. Mechanical vapour compression refrigerators have been used in many refrigeration and air-conditioning applications. However, increased global warming and environmental effect of chlorofluorocarbon has stimulated interest in the development of absorption refrigeration.

Vapour compression technologies require high grade energy for their operation, however, absorption refrigeration systems harness inexpensive waste heat, solar, etc. The Hydrogen Diffusion Absorption Refrigeration cycle HDAR invented by the Swedish engineers von Platen and Munters [1] has been recognized as one of the most promising technologies for refrigeration and cooling production. The corresponding thermodynamic cycle is based on refrigerant/absorbent pair mixture as working fluids and hydrogen gas for pressure equalization. A thermally driven bubble pump, which can be powered by waste heat or solar thermal energy, is used to lift the liquid solution. As a result of the absence of any mechanical moving part, the refrigerator is silent and very reliable [2] in addition of an economical and natural relative cycle.

The most used working fluid for this called hydrogen diffusion absorption refrigerator, manufactured and commercialised by Electrolux AB Sweden (today Dometic AB) [3], is the ammonia/water system with ammonia as refrigerant, water as absorbent and hydrogen as auxiliary gas [4, 5].

Over the years, numerous researches in this field have been done and a lot more is still undergoing. Works were mainly focused on thermodynamic modelling, finding new working fluids and improving the heat and mass transfers in mainly components of the DAR. Kouremenos et al. [6] examined the possibility of using helium instead of hydrogen as inert gas. They found that this gas behaves in a similar manner as hydrogen. Srikhirin et al. [7] developed a mathematical model of the cycle with ternary mixture ammonia/water/helium. The performance of the bubble pump was obtained from a simple experiment. This model was validated using experimental tests. Zohar et al. [8] also compared the COP of two cycle configurations, and investigated the influence of the generator and bubble pump configuration on the cycle performance [9]. A parametric study shows the best performances would be obtained with an ammonia mass concentration of 30% for the rich solution and 10% for the weak solution. In reference [10] Ben Ezzine et al. presented an experimental investigation of air-cooled DAR operating with light hydrocarbon mixture (C4/C9) and helium as inert gas. They produced cold at temperatures between −10 and +10 °C for a driving temperature in the range of 120–150 °C. Zohar et al. [11] examined numerically the performance of a DAR system working with an organic absorbent (DMAC-dimethylacetamide), five different refrigerant and helium as

ISSN 2356-5608

inert gas. Ben Ezzine et al. [12] investigated the feasibility of a DAR operating with the working fluid system DMAC-R124-He and coupled to a solar collector. The results indicated that at the same driving temperature (140 °C), the COP of the DAR system working with R124-DMAC was equal to 0.32 (maximum value) that was approximately 50% higher than that of the ammonia water refrigerator. Moreover, the lowest evaporation temperature was obtained as −14.8 °C at the driving temperature of 180 °C.

In this paper, the performance of a single pressure hydrogen diffusion absorption refrigeration cycle operating with ammonia-water mixture as working fluids and hydrogen as auxiliary inert gas has been analyzed by numerical simulation. The developed model is then used to investigate the effects of different operating parameters on the system performances.

II. Working Principal

A single pressure hydrogen diffusion absorption refrigerator is shown schematically in Fig. 1. The system consists, basically, of an absorber, an evaporator-gas heat exchanger, a rectifier, a condenser, a solution heat exchanger and a generator where the boiler and the bubbles pump are combined. The rich solution (6) leaving the absorber flows to the generator where it is heated causing the evaporation of some ammonia refrigerant. The resulting vapour bubbles rise in the tube. These vapour bubbles, which are separated by small liquid slugs, occupy the complete cross- section of the tube due to its small diameter. Each bubble acts as a gas piston and lifts the corresponding liquid slug to the top of the pump tube. Usually the vapour leaving the generator (10) contains a quantity of absorbent (H_2O). This vapour is then purified in the rectifier. The ammonia vapour (1) is then liquefied in the condenser. The liquid refrigerant (2) passes to the evaporator top. Since the evaporator is charged with hydrogen, the partial pressure of refrigerant decreases. It results that the ammonia evaporates at law temperature. As long as the refrigerant continues to evaporate, its partial pressure is rising. The resulting NH_3/hydrogen vapour mixture (5) flows out of the evaporator into the absorber which is continuously cooled and where the NH_3 weak solution absorbs the NH_3 from the vapour phase and forms an NH_3/H_2O rich solution (6).

III. Methodology of the Simulation

A. Modelling

The performance equations for the components considering mass and energy balances are established as follows.

Generator

Total mass balance, ammonia mass balance, and energy balance of the HDAR generator are expressed as follows:

$$\dot{m}_7 + \dot{m}_{11} = \dot{m}_8 + \dot{m}_{10} \quad (1)$$

$$\xi_r.\dot{m}_7 + \xi_{11}.\dot{m}_{11} = \xi_w.\dot{m}_8 + \psi_{10}.\dot{m}_{10} \quad (2)$$

$$\dot{Q}_{Gen} + \dot{m}_7.H_7 + \dot{m}_{11}.H_{11} = \dot{m}_8.H_8 + \dot{m}_{10}.H_{10} \quad (3)$$

The weak solution temperature T_8 leaving the generator is the highest temperature in the cycle. The leaving liquid solution and the vapor are in saturated state and at the same temperature, i.e.

$$T_8 = T_{10} \quad (4)$$

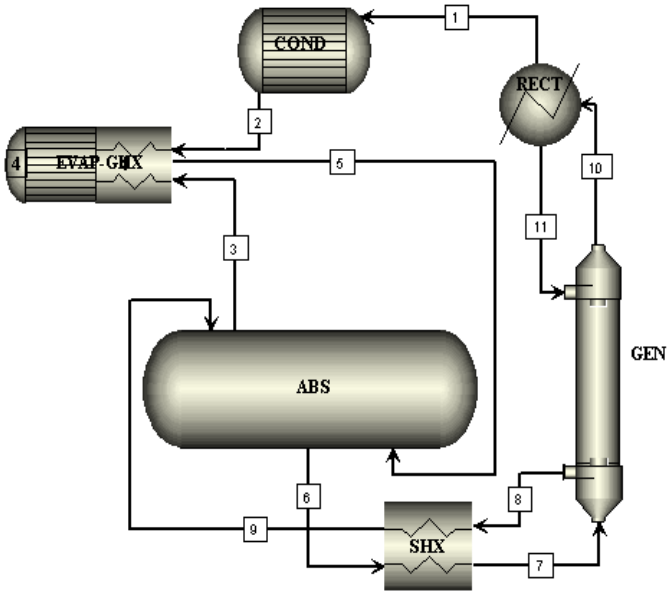

Fig. 1 Schematic view of the Diffusion Absorption Refrigeration Machine

Modeling for the Absorber

Total mass balance, ammonia mass balance, and the heat released by the exothermic process and rejected to the environment medium are expressed as follows:

$$\dot{m}_{5,H2} = \dot{m}_{3,H2} \quad (11)$$

$$\dot{m}_{5,NH3} + \dot{m}_9 = \dot{m}_{3,NH3} + \dot{m}_6 \quad (12)$$

$$\dot{m}_{5,NH3} + \xi_w.\dot{m}_9 = \dot{m}_{3,NH3} + \xi_r.\dot{m}_6 \quad (13)$$

$$\dot{Q}_{Abs} + \dot{m}_6.H_6 + \dot{m}_{3,NH3}.H_{3,NH3} + \dot{m}_{3,H2}.H_{3,H2} = \dot{m}_9.H_9 + \dot{m}_{5,NH3}.H_{5,NH3} + \dot{m}_{5,H2}.H_{5,H2} \quad (14)$$

Since the condenser has the same cooling medium, we assume that the same temperature difference prevails between the cooling medium and the exiting condensate, i.e.

$$T_9 = T_2 = T_C + \Delta T_{Cond} \quad (15)$$

The ammonia rich solution (9) leaving the absorber is in sub-cooled state.

To characterize absorption process absorber effectiveness is defined as the ratio between the quantities of refrigerant

absorbed to the maximum refrigerant quantities that can be absorbed in the same operating conditions.

$$Eff^{G}_{Abs} = \frac{\dot{m}_{5,NH3} - \dot{m}_{3,NH3}}{\dot{m}_{5,NH3} - (\dot{m}_{3,NH3})_{min}} \quad (16)$$

$$Eff^{L}_{Abs} = \frac{\xi_r.\dot{m}_6 - \xi_w.\dot{m}_9}{\xi_{rMax}.\dot{m}_{6Max} - \xi_w.\dot{m}_9} \quad (17)$$

Where $\xi_{rMax}, \dot{m}_{6Max}$ and $(\dot{m}_{3,NH3})_{min}$ are defined as the thermodynamic limits of the absorption process in the bottom and top of the absorption column. In fact, ξ_{rMax}, is the highest NH_3 mass fraction that can be contained in the rich solution and which can be reached when the thermodynamic equilibrium in the absorber's bottom is established at the partial pressure of the refrigerant leaving the evaporator. In such condition mass flow rate of the rich solution reaches its maximum value $\dot{m}_{6Max}$, finally $(\dot{m}_{3,NH3})_{min}$ is the lowest mass flow rate of the NH_3 residual in the gas mixture leaving the top the absorber and which can be reached when the gas mixture is in equilibrium with the weak solution (9) at the same temperature.

Modeling for the Evaporator-gas heat exchanger

Contrary to conventional two pressure absorption refrigeration systems when refrigerant is evaporated at constant evaporation low pressure, the evaporation process in hydrogen based triple fluid diffusion absorption refrigeration system is effectuated between two refrigerant partial pressure. At the evaporator entrance, the sub-cooled liquid refrigerant (2) leaving the condenser at the total system pressure arrives at the evaporator entrance, relaxes into the hydrogen and NH_3 mixture and the result is that the partial pressure of the sub-cooled liquid NH_3 drops and it starts to evaporate at low temperatures. More the liquid evaporates while traversing the evaporator more the refrigerant partial pressure in the vapor phase increases. Therefore temperature through the evaporator-gas heat exchanger increases and the evaporator-gas heat exchanger outlet temperature T_5 is then fixed.

Many factors affect the evaporation process such as refrigerant mass flow, NH_3 partial pressure, temperature, absorber effectiveness, etc. The partial pressure of NH_3 in the gas mixture is defined as:

$$P_{Part} = \frac{\dot{n}^{g}_{NH3}}{\dot{n}^{g}_{NH3} + \dot{n}_{H2}} * P_{Syst} \quad (18)$$

$$P_{PartMax} = \frac{\dot{n}^{g}_{5,NH3}}{\dot{n}^{g}_{5,NH3} + \dot{n}_{5,H2}} * P_{Syst} \quad (19)$$

$$P_{PartMin} = \frac{\dot{n}^{g}_{3,NH3}}{\dot{n}^{g}_{3,NH3} + \dot{n}_{3,H2}} * P_{Syst} \quad (20)$$

The lowest temperature attempted in the evaporator's top can be calculated when $P_{PartMin}$ is known. Total mass balance, ammonia mass balance, and energy balance on the HDAR evaporator are expressed as follows:

$$\dot{m}_{5,H2} = \dot{m}_{3,H2} \quad (21)$$

$$\dot{m}_{3,NH3} + \dot{m}_2 = \dot{m}_{5,NH3} \quad (22)$$

$$\dot{Q}_{Evap} + \dot{m}_2.H_2 + \dot{m}_{3,NH3}.H_{3,NH3} + \dot{m}_{3,H2}.H_{3,H2} = \dot{m}_{5,NH3}.H_{5,NH3} + \dot{m}_{5,H2}.H_{5,H2} \quad (23)$$

Modeling for the Rectifier

The vapor leaving the generator is not pure refrigerant; it contains yet a small amount of absorbent. It is purified by a partial condensation in the cooled rectifier. Total mass balance, NH_3 mass balance, and energy balance are expressed as follows:

$$\dot{m}_1 + \dot{m}_{11} = \dot{m}_{10} \quad (24)$$

$$\dot{m}_1 + \xi_{11}.\dot{m}_{11} = \psi_{10}.\dot{m}_{10} \quad (25)$$

$$\dot{Q}_{Rect} + \dot{m}_1.H_1 + \dot{m}_{11}.H_{11} = \dot{m}_{10}.H_{10} \quad (26)$$

The refrigerant vapor leaves the rectifier in a saturated state (location 1). A temperature difference of ΔT_{Rect} = 2°C is assumed between exiting vapor (10) and refluxing liquid (11), i.e.

$$T_{10} = T_{11} + \Delta T_{Rect} \quad (27)$$

B. Cycle performance

Coefficient of performance is defined as:

$$COP = \frac{\dot{Q}_{Evap}}{\dot{Q}_{Gen}} = \frac{\dot{Q}_{Evap}}{\dot{Q}_B + \dot{Q}_{BP}} \quad (28)$$

The correspondent theoretical reversible cycle is assumed to operate between three thermal sources, a cold source at TF = $T_4 = T_{Min}$, a medium source at T_C and a driving heat source at $T_G = T_8$. The theoretical *COP* is then:

$$COP_{rev} = \frac{T_F(T_G - T_C)}{T_G(T_C - T_E)} \quad (29)$$

The cycle efficiency writes:

$$\eta = \frac{COP}{COP_{rev}} \quad (30)$$

The circulation ratio is defined as the ratio between the rich solution mass flow rate and that of the refrigerant:

$$f = \frac{\dot{m}_6}{\dot{m}_1} \quad (31)$$

C. Numerical resolution

The numerical simulation model is constituted of a large set of non-linear equations (mass and energy balances and

thermodynamic properties equations) is simultaneously solved using a FORTRAN program based on the CONLES algorithm [23, 24].

IV. Results and Discussion

The performance of hydrogen based ammonia-water diffusion absorption cycle is simulated in two cooling modes, viz. water cooling and air cooling.

The cycle is then simulated in the two cooling medium cases, 27°C for water-cooling and 35°C for air-cooling. Simulation is performed for three driving temperature 90°C, 120°C and 140°C for water-cooled cycle and 120°C,140°C and 180 °C for air-cooled machine. Simulation's inputs and calculation results of the NH_3/H_2O diffusion-absorption refrigeration cycle for the two cases are presented in Table 1.

In table 2 the exchanged heat rates, the circulation ratio and the coefficient of performance of the various configurations are given. We remark that in the case of water cooling, driving heat temperatures above 120°C are not necessary, unlike the case of air cooling where higher temperatures are needed to enhance the coefficient of performance.

TABLE I

BASE CASE SIMULATION RESULTS

	Water cooled, T_C = 27 °C			**Air cooled, T_C = 35 °C**		
Parameter \ T_{Max}	90°C	120°C	140°C	120°C	140°C	180°C
P_{Syst} (bar)	14.73	14.73	14.73	18.35	18.35	18.35
$P_{PartMax}$ (bar)	5.15	5.15	5.15	5.15	5.15	5.15
$P_{PartMin}$ (bar)	3.438	1.408	0.734	2.56	1.42	0.36
P_{Part3} (bar)	3.828	2.375	1.917	3.156	2.32	1.58
T_1 (°C)	47.25	47.25	47.25	53.	53.	53.
T_2 (°C)	37.	37.	37.	45.	45.	45.
T_3 (°C)	37.	37.	37.	45.	45.	45.
$T_4 = T_{Min}$ (°C)	-3	-14.8	-19.8	-7.9	-15.4	-24
T_5 (°C)	5.	5.	5.	5.	5.	5.
T_6 (°C)	37.	37.	37.	45.	45.	45.
T_7 (°C)	78.9	86.48	91.1	100.8	106.	115.2
T_{10} (°C)	88.	108.	138.	118.	138.	178.
T_{11} (°C)	86.	106.	136.	116.	136.	176.
ξ_r (%)	50.8	48.	46.2	61.1	59.3	56.7
ξ_w (%)	44.7	30.3	21.5	52.4	43.4	30.6
$\dot{m}_1$ (g/s)	2.12	1.3	1.24	2.932	1.894	1.61
$\dot{m}_{5(NH3)}$ (g/s)	6.09	2.03	1.72	6.26	3.01	2.12
$\dot{m}_{5(H2)}$ (g/s)	1.322	0.44	0.36	1.876	0.9	0.62
$\dot{m}_{3(NH3)}$ (g/s)	3.97	0.72	0.48	3.33	1.12	0.51
$\dot{m}_{3(H2)}$ (g/s)	1.322	0.44	0.36	1.876	0.9	0.62
$\dot{m}_r$ (g/s)	19.67	5.3	4.08	20.36	8.63	5.03
$\dot{m}_w$ (g/s)	17.55	3.99	2.84	17.43	6.73	3.43

TABLE II

HEAT EXCHANGE RATES AND PERFORMANCES OF THE MACHINE.

Parameter \ T_{Max}	Water cooled, T_C = 27 °C			Air cooled, T_C = 35 °C		
	90°C	120°C	140°C	120°C	140°C	180°C
$\dot{Q}_{Evap}$ (W)	1000.	1000.	1000.	1000.	1000.	1000.
$\dot{Q}_{Gen}$ (W)	3964.	2767.2	3222.6	6104.7	4554.8	7517.
$\dot{Q}_{Abs}$ (W)	2119.2	1604.2	1623.4	2616.6	2026.7	1998.9
$\dot{Q}_{Cond}$ (W)	2357.4	1454.8	1386.4	3155.9	2037.7	1731.8
$\dot{Q}_{Rect}$ (W)	487.3	708.2	1212.6	1332.2	1490.3	4786.2
f	9.27	4.1	3.29	6.95	4.56	3.12
COP	**0.252**	**0.361**	**0.31**	**0.163**	**0.22**	**0.133**

V. Parametric Study on Performance

The variation of the coefficient of performance vs. the driving heat temperature for different absorber efficiencies in the base case air cooled DAR is presented in figure 2. When the absorber efficiency is constant, the COP firstly increases to a maximum value with driving temperature increasing and then diminishes. On the other hand, the coefficient of performance is largely affected by the absorber efficiency.

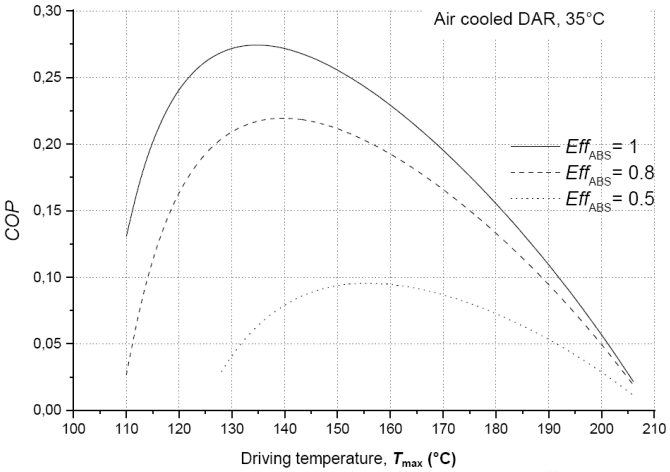

Fig. 2 COP vs. driving temperature for different absorber efficiencies

In figure 3 the evolution of the weak solution concentration exiting the generator with the driving heat temperature Tmax for air cooling is depicted. It's clear that the refrigerant mass fraction decreases with higher temperatures. This decreases is good for the absorption process in the absorber and then enhances the performance of the refrigerator. On the other hand, as presented in figure 4 which shows the heat rejected by rectification process vs. the maximum driving heat temperature Tmax. The rejected heat increase first slowly until a driving temperature of 140°C.

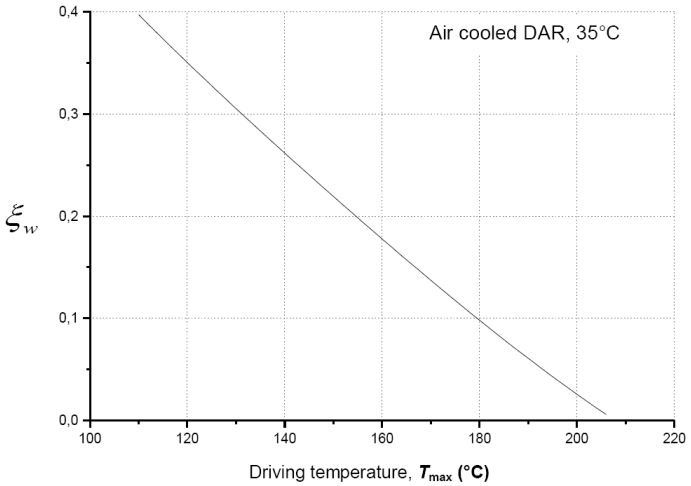

Fig. 3 Concentration of weak solution vs. driving temperature for constant absorber efficiency

The higher the driving temperature, the greater the rectification heat and consequently the decrease of the COP beyond the optimal temperature.

Figure 5 shows the variation of the circulation ratio, f as a function of the driving temperature for the two case of cooling medium temperatures, 27°C for water-cooling and 35°C for air-cooling. It can be deduced from this figure that the circulation ratio f increases rapidly as more as the driving temperature is decreasing. In general, it can be seen from the thermal coefficients that in order to obtain a higher operation efficiencies it is essential to operate the DAR cycle at lower circulation ratio, which implies higher values of Tmax and lower cooling medium temperatures. That same figure shows also that at absorber efficiency about 80%, the water-cooled DAR circulation ratio varied from 4.5 to 2.4 when Tmax was varied from 110°C to 200°C but in the air-cooled DAR, circulation ratio varied from 10.45 to 2.75 for the same operation conditions.

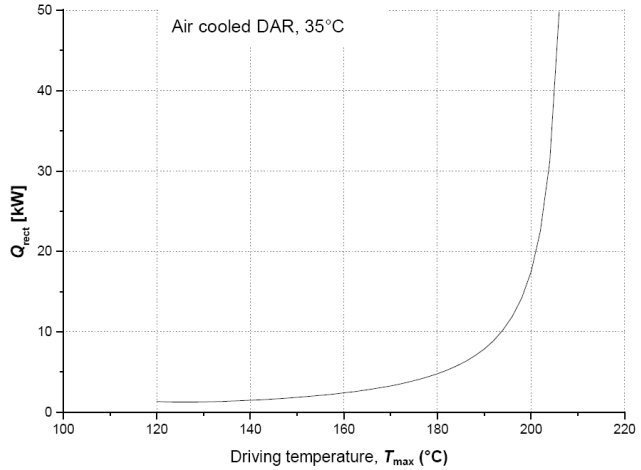

Fig. 4 Rejected heat from rectifier vs. Tmax

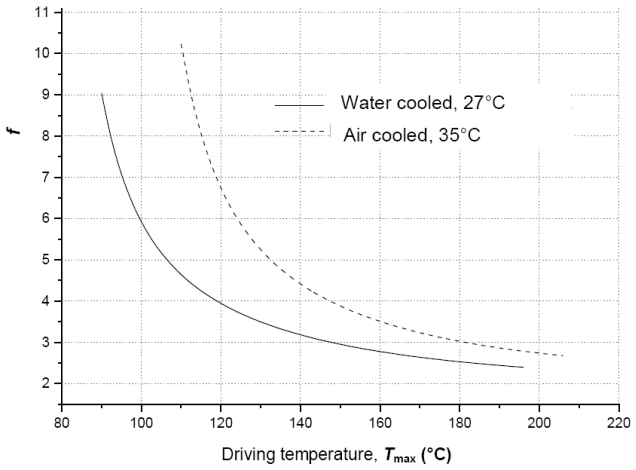

Fig. 5 Circulation ratio vs. driving temperature and cooling medium temperature

The last figure (Fig. 6) reports the investigation of the conjugate effect of the absorption temperature (resulting from varying cooling medium temperature) and the driving heat temperatures on the COP of the DAR for constant absorber efficiency. For each driving temperature (12, 140 and 160°C) the COP decreases rapidly when the temperature TC is increased. This shows again the predominant role of the absorber and how it largely affects the performance of the DAR.

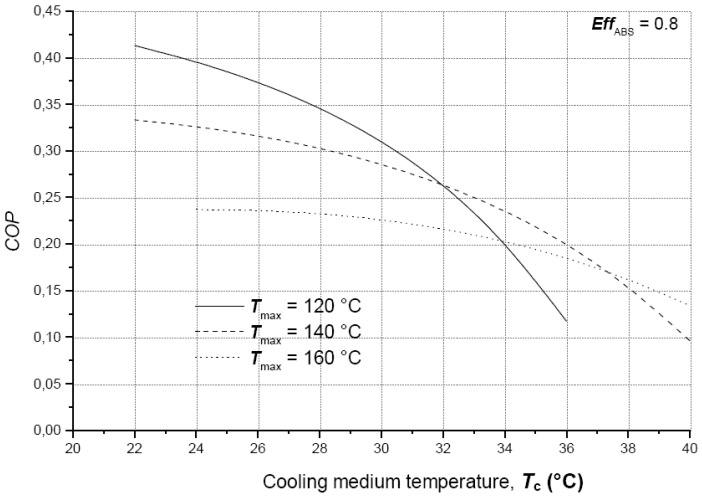

Fig. 6 COP vs. cooling medium and driving heat temperature

VI. CONCLUSIONS

A thermodynamic model for ammonia-water-hydrogen DAR cycle is developed and the system performances are analyzed parametrically by computer simulation. With the thermodynamic model developed, the numerical simulation shows that for absorber effectiveness of 80%, the optimum driving temperature for the air-cooled DAR cycle is around 140°C, and the corresponding COP reaching 0.22. In comparison, the water-cooled performance cycle is better with a higher COP is up to 0.36 and a lower optimum driving temperature around 120°C.

Parametric results show that the driving temperature and the absorber efficiency have the largest effect on the coefficient of performance and the minimum evaporation temperature.

NOMENCLATURE

COP	coefficient of performance
$\dot{m}$	mass flow rate (Kg.s-1)
$\dot{n}$	molar flow (mol.s-1)
$\dot{Q}$	heat flow (KW)
H	enthalpy (KJ.Kg-1)
P	pressure (bar)
T	temperature (°C)
ΔT	heat exchanger pinch
SRC	condenser sub-cooling
x, y	liquid and vapor molar composition
DAR	diffusion absorption refrigerator

Greek letters

ξ	NH3 solution mass fraction
ψ	NH3 gas mass fraction

Exponents

v ,g	*gas phase*

Subscripts

Abs	absorber
Cond	condenser
Evap	evaporator
Gen	generator
Rect	rectifier
SHX	solution heat exchanger
H2	hydrogen
Min	minimal
Max	maximal
Part	*partial pressure*
r	rich solution
w	weak solution
1,2....14	system's state point

REFERENCES

[1] B.C. Von Platen, C.G. Munters. US Patent 1, 685,764, 1928.

[2] A. Koyfman, M. Jelinek, A. Levy, I. Borde, An experimental investigation of bubble pump performance for diffusion absorption refrigeration system with organic working fluids, Applied Thermal Engineering 23 (2003) 1881-1894.

[3] Domestic © 2003, www.dometic.com (formerly known as Electrolux in Europe).

[4] U. Jakob, U. Eicker, D. Schneider, A.H. Taki, M.J. Cook, Simulation and experimental investigation into diffusion absorption cooling machines for air conditioning applications, Applied Thermal Engineering (2007).

[5] A. Zohar, M. Jelinek, A. Levy, I. Brode, Numerical investigation of a diffusion-absorption refrigeration cycle, Int. J. Refrigeration 28(4) (2005) 515–525.

[6] D.A. Kouremenos, A. Stegou-Sagia, Use of helium instead of hydrogen in inert gas absorption refrigeration, International Journal of Refrigeration, 11 (1988), pp. 6-341.

[7] P. Srikhirin, S. Aphornratana, Investigation of a diffusion absorption refrigerator. Applied Thermal Engineering, 22 (2002), pp. 1181-1193.

[8] A. Zohar, M. Jelinek, A. Levy, I. Brode, The influence of diffusion absorption refrigeration cycle configuration on the performance, Applied Thermal Engineering 27 (2007) 2213-2219.

[9] A. Zohar, M. Jelinek, A. Levy, I. Borde, The influence of the generator and bubble pump configuration on the performance of diffusion absorption refrigeration (DAR) system, Int. J. Refrig. 31 (2008) 962-969.

[10] N. Ben Ezzine, R. Garma, M. Bourouis, A. Bellagi, Experimental studies on bubble pump operated diffusion absorption machine based on light hydrocarbons for solar cooling, Renew. Energ. 35 (2010) 464-470.

[11] A. Zohar, M. Jelinek, A. Levy, I. Borde, Performance of diffusion absorption refrigeration cycle with organic working fluids, Int. J. Refrigeration, 32 (2009), pp. 1241–1246.

[12] N. Ben Ezzine, R. Garma, A. Bellagi, A numerical investigation of a diffusion absorption refrigeration cycle based on R124-DMAC mixture for solar cooling. Energy, 5 (2010), 1874-1883.

[13] Q. Wang, L. Gong, J.P. Wang, T.F. Sun, K. Cui, G.M. Chen, A numerical investigation of a diffusion absorption refrigerator operating with the binary refrigerant for low temperature applications, Appl. Therm. Eng., 31 (2011), pp. 1763–1769.

[14] J. Chen, K.J. Kim, K.E. Herold, Performance enhancement of a diffusion-absorption refrigerator, Int. J. Refrigeration 19 (3) (1996) 208-218.

[15] Da-Wen Sun, Comparison of the performance of NH3-H2O, NH3-LiNO3 and NH3-NaSCN absorption refrigeration systems, Energy Conversion Management, 39(5) (1998) 357-368.

[16] R. Saravanan, M.P. Maiya, Experimental analysis of a bubble pump operated H2O-LiBr vapour absorption cooler, Applied Thermal Engineering 23 (2003) 2383-2397.

[17] Y. He, G. Chen, Experimental study on an absorption refrigeration system at low temperatures, International Journal of Thermal Sciences, 46 (2007) 294-299.

[18] I. Borde, M. Jelinek, N.C. Daltrophe, Working fluids for absorption refrigeration systems based on R124 and organic absorbents, Intern. J. Refrig. 20(4) (1997) 256–266.

[19] I. Borde, M. Jelinek, N.C. Daltrophe, Absorption system based on refrigerant R134a, International Journal of Refrigeration, 18(6) (1995) 387–394.

[20] M. Barhoumi, A. Snoussi, N. Ben Ezzine, A. Bellagi, Modelling of the thermodynamic properties of the ammonia –water mixture, International Journal of Refrigeration 27(3) (2004) 271-283.

[21] Kh. Mejbri, N. Ben Ezzine, A. Bellagi, Modélisation numérique des propriétés thermodynamiques du mélange frigorifique ammoniac-eau, Journal de la Société Chimique de Tunisie, 6(2) (2004) 213-228.

[22] G. Alefeld, R. Radermacher, Heat conversion systems, CRC Press, Boca Raton, FL, 1993.

[23] N. Ben Ezzine, Kh. Mejbri, M. Barhoumi, A. Bellagi, Thermodynamic analysis and multi-parametric optimisation of double effect absorption chiller , International Journal of Exergy, Vol. 3, N°1, 2006, 68-86.

[24] M. Shacham, Int. J. Num. Methods in Engineering, 23 (1986), pp.1455-1481.